Journal of Physics B: Atomic, Molecular and Optical Physics

PAPER

High-accuracy calculations of the lowest eleven Rydberg ^2P states of the Li atom

IOP Publishing Journal of Physics B: Atomic, Molecular and Optical Physics
J. Phys. B: At. Mol. Opt. Phys. **54** (2021) 085003 (16pp) https://doi.org/10.1088/1361-6455/abee97

High-accuracy calculations of the lowest eleven Rydberg ^2P states of the Li atom

Saeed Nasiri[1,*], Toreniyaz Shomenov[1], Sergiy Bubin[1] and Ludwik Adamowicz[2,3,4]

[1] Department of Physics, Nazarbayev University, Nur-Sultan 010000, Kazakhstan
[2] Department of Chemistry and Biochemistry, University of Arizona, Tucson, AZ 85721, United States of America
[3] Department of Physics, University of Arizona, Tucson, AZ 85721, United States of America
[4] Interdisciplinary Center for Modern Technologies, Nicolaus Copernicus University, ul. Wileńska 4, Toruń, PL 87-100, Poland

E-mail: saeed.nasiri@nu.edu.kz, toreniyaz.shomenov@nu.edu.kz, sergiy.bubin@nu.edu.kz and ludwik@arizona.edu

Received 28 December 2020, revised 22 February 2021
Accepted for publication 15 March 2021
Published 4 May 2021

Abstract

Highly accurate calculations are reported for the eleven lowest states of the ^2P Rydberg series ($1s^2np^1, n = 2, \ldots, 12$) of the lithium atom. The nonrelativistic wave functions of the states are expanded in terms of up to 16 000 all-electron explicitly correlated Gaussian (ECG) basis functions. The ECG exponential parameters are variationally optimized using a method that employs the analytical energy gradient determined for the parameters. The finite-nuclear-mass effects of the ^{6}Li and ^{7}Li isotopes are explicitly included in the nonrelativistic variational calculations. The results also include the leading relativistic and quantum electrodynamics energy corrections computed using the framework of perturbation theory. The calculated interstate transition energies are compared with the available experimental data. The ^{6}Li–^{7}Li isotope shifts of the transition energies are determined.

Keywords: all-electron explicitly correlated Gaussian function, relativistic corrections for few-electron atoms, Rydberg spectrum of lithium atom

(Some figures may appear in colour only in the online journal)

1. Introduction

Since the beginning of quantum mechanics, quantitative studies of atomic energy levels have contributed many important results to the atomic physics and, in particular, atomic Rydberg systems [1]. The data obtained have enhanced our understanding of the atomic electronic structure and of other atomic properties. With the advancement of computational approaches, it has been possible to develop more accurate theoretical models for the electronic structure of atoms. Through experimental and theoretical studies, it has been shown that highly excited Rydberg atoms possess some unusual properties that can be controlled by state selection and the application of external electromagnetic fields [2]. With the discovery of these properties in recent decades, new and interesting applications have been proposed for Rydberg atoms [3].

Back in 1982, Richard Feynman postulated that in order to accurately simulate the behavior of a quantum system in a reasonable amount of time, a new generation of computers called quantum computers needed to be built [4]. In recent decades, superconductors, trapped ions, quantum dots, neutral atoms, photons, and spins in solid-state hosts have been examined for use in quantum information processing [5, 6]. The use of neutral Rydberg atoms as qubits boasts several interesting characteristics. Atoms of a particular isotope of an element are quantum systems that can be readily prepared in well-defined, stable, and identical quantum states. Although the application of atoms is limited by the tunability of their properties, Rydberg atoms offer strong and tunable atomic

* Author to whom any correspondence should be addressed.

interactions that can be adjusted by selecting states with different principal quantum numbers or orbital angular momenta. These features make Rydberg atoms highly desirable candidates for the development of memory units for quantum computers [5–7].

The accuracy of the results obtained using theoretical models is influenced by two key factors. The first is related to the use of the Born–Oppenheimer (BO) approximation in the calculations. Due to the dependence of the properties of Rydberg atoms on the mass of the nucleus, the coupling of the motions of the nucleus and the electrons should be accounted for in high-accuracy calculations (see reference [6]), i.e. the BO approximation should not be assumed at the start of the calculations. To our knowledge, such non-BO high-accuracy atomic calculations have only been performed by our group [8, 9]. The second key factor in achieving high-accuracy results from atomic calculations is the selection of an appropriate basis function for expanding the wave function of the studied states of the system. Explicitly correlated basis functions are likely to be the best choice for performing atomic ground- and excited-state calculations. As such functions explicitly depend on inter-electron distances, they allow for a very accurate description of the electronic correlation effects. Hylleraas-type (Hy) functions and explicitly correlated Gaussian (ECG) functions have been the most popular correlated basis functions used in high-accuracy atomic calculations. However, the former functions, despite their superb accuracy, cannot easily be extended to calculate the states of atomic systems with more than three electrons. The Gaussian functions do not have these limitations, but they are not as efficient as the Hy functions in describing the behavior of the wave function near the particle coalescence points, and have less favourable long range behavior. The deficiency of the Gaussian functions, that they do not fulfill the so-called Kato cusp conditions, can be remedied by using larger expansions of the wave function in terms of these functions. Employing a larger number of well-optimized basis functions to calculate the ground and excited atomic states not only improves the accuracy of the total atomic energy but also the accuracy of the expectation values of other important atomic properties. However, properties represented by operators with singularities may still show considerably worse convergence than that of the total energy. This, for example, applies to operators involving one- and two-electron Dirac delta functions, $\delta\left(\mathbf{r}_{ij}\right)$, and the operators describing the relativistic correction to the kinetic energy, which contain the fourth power of the linear momenta. The convergence rate of the expectation values of such operators with the number of basis functions may be significantly slower than the convergence of the expectation value of the Hamiltonian. In some cases, this slow convergence can be overcome by adopting regularization techniques that employ expectation value identities that allow a more accurate determination of the expectation values for the eigenstates of the Hamiltonian.

One of the aims of this work is to implement expectation value identities involving singular operators that appear in the calculation of the leading relativistic corrections for atomic P states. As mentioned above, the operator regularization approach accelerates the convergence of the expectation values of singular operators in terms of the number of basis functions. Thus, one can use an expansion of the wave function that already provides satisfactory convergence for the total energy, but not yet for the expectation value of a singular operator, to calculate its expectation value using an identity. That may be particularly important for highly excited states, where the basis set convergence usually becomes notably worse than for the lower-energy states.

Although some P states of the lithium atom have been previously studied using explicitly correlated methods by other groups [10–28], those works have been limited to just a couple of the lowest states. There are only two works where highly excited P states have been considered, one by the present authors [27] and one by Wang *et al* [29]. It is important to note that the use of the non-BO approach from the start (i.e. non-perturbatively) in the present calculations sets the present work apart from previous calculations by other groups, where the non-relativistic wave function and the corresponding energy were generally obtained by assuming an infinite mass of the nucleus, while the corrections due to the finite nuclear mass were calculated using perturbation theory. The use of the non-BO nonrelativistic wave function also facilitates the automatic inclusion of recoil effects when the relativistic corrections are computed.

2. Method

The basic all-electron ECG basis functions used to construct the P-state wave functions in the present work have the following form (for more information see references [30, 31]):

$$\phi_k = z_{i_k} \exp\left[-\mathbf{r}'\left(A_k \otimes I_3\right)\mathbf{r}\right], \tag{1}$$

where $\mathbf{r}$ is a $3n$ vector column of the electron coordinates (referenced to the nucleus),

$$\mathbf{r} = \begin{pmatrix} \mathbf{r}_1 \\ \mathbf{r}_2 \\ \mathbf{r}_3 \end{pmatrix},$$

z_{i_k} is the z-coordinate of the ith electron, i_k is an adjustable integer parameter (specific to each basis function k), A_k is an $n \times n$ real symmetric matrix, $\otimes$ is the Kronecker product, and I_3 is a 3×3 identity matrix. The prime symbol denotes the matrix/vector transpose. The Gaussian basis function (1) is square integrable if matrix A_k is positive definite. To assure this requirement, A_k is represented by the Cholesky-factored form, $A_k = L_k L_k'$, where L_k is a lower triangular matrix. The A_k matrix given in this form is always positive definite, regardless of the values of the L_k matrix elements. Thus, the elements of L_k can be varied without any constraints from ∞ to $-\infty$.

In the present calculations, we use the spin-free formalism to ensure the correct permutational symmetry properties. For this purpose, an appropriate permutational symmetry projector is constructed and applied to each

basis function (1). In constructing the symmetry projector, the standard procedure involving Young operators (see references [32, 33]) is used. In the case of the ^2P states of lithium, the permutation operator can be chosen in the form $Y = (1 + P_{12})(1 - P_{23})$, where P_{ij} denotes the permutation of the spatial coordinates of the ith and jth electrons (particle 0 is the nucleus). More details about the generation of the wave function and its variational optimization can be found in references [27, 31].

In the nonrelativistic (nr) variational calculations, the Hamiltonian is obtained by separating the atom's center-of-mass motion from the nonrelativistic laboratory-frame Hamiltonian. This separation is rigorous and reduces the four-particle problem of the Li atom to a three pseudoparticle problem represented by the following 'internal' Hamiltonian, expressed in terms of $\mathbf{r}_i$'s (atomic units are assumed throughout):

$$H_{\rm nr}^{\rm int} = -\frac{1}{2}\left(\sum_{i=1}^{3}\frac{1}{\mu_i}\nabla_{\mathbf{r}_i}^2 + \sum_{i=1}^{3}\sum_{j\neq i}^{3}\frac{1}{m_0}\nabla'_{\mathbf{r}_i}\nabla_{\mathbf{r}_j}\right) + \sum_{i=1}^{3}\frac{q_0 q_i}{\mathbf{r}_i} + \sum_{i=1}^{3}\sum_{j<i}^{3}\frac{q_i q_j}{\mathbf{r}_{ij}}. \quad (2)$$

Here, $q_0 = 3$ is charge of the nucleus, $q_i = -1$ ($i = 1, 2, 3$) are the electron charges, m_0 is the nuclear mass ($m_0 = 12\,786.3933$ for ^{7}Li and $m_0 = 10\,961.898$ for ^{6}Li), $\mu_i = m_0 m_i/(m_0 + m_i)$ is the reduced mass of the electron i ($m_1 = m_2 = m_3 = 1$), and $r_{ij} = |\mathbf{r}_j - \mathbf{r}_i|$ are the distances between the (pseudo)electrons. The calculations involving the nonrelativistic Hamiltonian $H_{\rm nr}^{\rm int}$ can be carried out for both finite and infinite masses of the Li nucleus. They yield the nonrelativistic ground- and excited-state energies ($E_{\rm nr}$) and the corresponding wave functions. Both the energy and the wave function depend on the mass of the nucleus. In this work, we report both the finite-mass and infinite-mass results. The Hamiltonian (2) can also be conveniently written in a compact matrix form [8] as:

$$H_{\rm nr}^{\rm int} = -\nabla'_{\mathbf{r}}\mathbf{M}\nabla_{\mathbf{r}} + \sum_{i=1}^{3}\frac{q_0 q_i}{\mathbf{r}_i} + \sum_{i=1}^{3}\sum_{j<i}^{3}\frac{q_i q_j}{\mathbf{r}_{ij}}, \quad (3)$$

where

$$\nabla_{\mathbf{r}} = \begin{pmatrix}\nabla_{\mathbf{r}_1}\\ \nabla_{\mathbf{r}_2}\\ \nabla_{\mathbf{r}_3}\end{pmatrix}$$

is a nine-component gradient vector and $\mathbf{M} = M \otimes I_3$ is the Kronecker product of a 3×3 matrix M and the 3×3 identity matrix I_3. The matrix M has diagonal elements $1/(2\mu_1)$, $1/(2\mu_2)$, and $1/(2\mu_3)$, while all the off-diagonal elements are equal to $1/(2m_0)$.

The nonrelativistic energy, even obtained using a very accurate, well optimized wave function, is insufficient to calculate the total and transition energies of the atomic ground and excited states with an accuracy comparable to the available experimental results. The relativistic and quantum electrodynamics (QED) effects must also be included in the calculations. The approach that is the most practical and most frquently used to account for the relativistic and QED effects in light atoms is to expand the total energy in powers of the fine-structure constant, α [34, 35]:

$$E_{\rm tot} = E_{\rm nr} + \alpha^2 E_{\rm rel}^{(2)} + \alpha^3 E_{\rm QED}^{(3)} + \alpha^4 E_{\rm HQED}^{(4)} + \ldots, \quad (4)$$

where $E_{\rm nr}$ is the nonrelativistic energy of the state being considered, the second term, $\alpha^2 E_{\rm rel}^{(2)}$, represents the leading relativistic corrections, the third term, $\alpha^3 E_{\rm QED}^{(3)}$, represents the leading QED corrections, and the fourth term, $\alpha^4 E_{\rm HQED}^{(4)}$, represent the higher-order QED corrections. Each of these terms is evaluated as an expectation value of some effective operator that represents the calculated term. $E_{\rm rel}^{(2)}$ is calculated as the expectation value of the Dirac–Breit Hamiltonian in the Pauli approximation, $H_{\rm rel}$ [36, 37]. In this study, the relativistic correction for the P-states, $H_{\rm rel}$, contains the following terms:

$$H_{\rm rel} = H_{\rm MV} + H_{\rm D} + H_{\rm OO} + H_{\rm SS}, \quad (5)$$

where $H_{\rm MV}$, $H_{\rm D}$, $H_{\rm OO}$, and $H_{\rm SS}$ are operators that are commonly interpreted as the mass–velocity, Darwin, orbit–orbit, and spin–spin corrections, respectively. The explicit form of these operators in the internal coordinates can be found in our previous works [38, 39]. It should be mentioned that, due to the use of a finite nuclear mass in the nonrelativistic Hamiltonian, the recoil effects are directly included in the calculations of the relativistic correction. In general, for non-singlet states of atoms, $H_{\rm rel}$ should also contain a term describing the spin–orbit interaction. In this work, however, it was not included. The experimental data show that the fine-structured splits for the lithium atom are small. In fact, for the excited nP states ($n > 2$) they get progressively smaller (a few hundredths of a wavenumber) and essentially vanish in the limit of high n. As we are primarily concerned with the energy levels and transitions between Rydberg states, the missing contribution due to the spin–orbit term is not expected to have a particularly notable effect on the accuracy of our calculations.

The $E_{\rm QED}^{(3)}$ term in (4) represents the leading QED correction. For an atomic system, it takes into account the two-photon exchange, the vacuum polarization, and the electron self-energy effects. The explicit form of the operator is:

$$H_{\rm QED} = \sum_{\substack{i,j=1\\ j>i}}^{3}\left[\left(\frac{164}{15} + \frac{14}{3}\ln\alpha\right)\delta(\mathbf{r}_{ij}) - \frac{7}{6\pi}\mathcal{P}\left(\frac{1}{r_{ij}^3}\right)\right] + \sum_{i=1}^{3}\left(\frac{19}{30} - 2\ln\alpha - \ln k_0\right)\frac{4q_0}{3}\delta(\mathbf{r}_i), \quad (6)$$

where the first sum represents the Araki–Sucher term [11, 40–43], while the principal value $\mathcal{P}\left(1/r_{ij}^3\right)$ is defined as:

$$\left\langle \mathcal{P}\left(\frac{1}{r_{ij}^3}\right)\right\rangle = \lim_{a\to 0}\left\langle \frac{1}{r_{ij}^3}\Theta(r_{ij} - a) + 4\pi(\gamma + \ln a)\delta(\mathbf{r}_{ij})\right\rangle. \quad (7)$$

In the last expression, $\Theta(\ldots)$ is the Heaviside step function and $\gamma = 0.577\,215\ldots$ is the Euler–Mascheroni constant.

The dominant part of the electron self-energy is the so-called Bethe logarithm, $\ln k_0$, which appears in expression (6).

Table 1. Comparison of the convergence of the expectation values of some singular operators for three selected Rydberg states of $^{\infty}$Li computed using the regularization technique (marked with a tilde) and using direct calculations (no tilde). All values are in atomic units.

State	Basis	$\langle \tilde{H}_{\rm MV} \rangle$	$\langle H_{\rm MV} \rangle$	$\langle \tilde{\delta}(\mathbf{r}_i) \rangle$	$\langle \delta(\mathbf{r}_i) \rangle$	$\langle \tilde{\delta}(\mathbf{r}_{ij}) \rangle$	$\langle \delta(\mathbf{r}_{ij}) \rangle$
$1s^2 2p^1$	6000	−77.505 654	−77.503 986	4.558 732 346	4.558 617 001	0.177 424 699	0.177 432 409
	7000	−77.505 640	−77.504 338	4.558 732 348	4.558 643 190	0.177 424 700	0.177 429 516
	8000	−77.505 630	−77.505 072	4.558 732 350	4.558 693 976	0.177 424 700	0.177 427 586
	9000	−77.505 624	−77.505 244	4.558 732 350	4.558 705 279	0.177 424 700	0.177 426 306
Ref. [28]	33 600	−77.505 616 73(9)		4.558 732 350 19(2)		0.177 424 6999(1)	
$1s^2 7p^1$	9000	−77.634 311	−77.626 752	4.567 779 196	4.567 246 971	0.177 896 659	0.177 961 446
	10 000	−77.634 174	−77.628 321	4.567 779 250	4.567 365 639	0.177 896 676	0.177 934 245
	11 000	−77.634 056	−77.630 790	4.567 779 286	4.567 550 718	0.177 896 682	0.177 911 928
	12 000	−77.634 043	−77.631 901	4.567 779 296	4.567 625 944	0.177 896 683	0.177 907 462
$1s^2 12p^1$	13 000	−77.637 128	−77.593 046	4.567 955 622	4.564 247 289	0.177 904 856	0.178 139 915
	14 000	−77.636 807	−77.595 332	4.56 795 6970	4.564 559 712	0.177 905 063	0.178 068 158
	15 000	−77.636 775	−77.603 093	4.567 958 235	4.565 213 610	0.177 905 145	0.178 047 780
	16 000	−77.636 757	−77.608 466	4.567 959 099	4.565 627 984	0.177 905 199	0.178 037 245

The main difficulty in computing the QED term for a multi-electron atomic system is to accurately calculate $\ln k_0$. It is known that the dominant contribution to $\ln k_0$ comes from the inner shell electrons. Therefore, at the lowest level of the approximation, the value of the Bethe logarithm determined for the $1s^2 2p^1$ state of the Li atom may be used to calculate the QED corrections for the higher states of this system. The Bethe logarithm for the Li $1s^2 2p^1$ state was calculated by Yan *et al* [21] and is adopted in our current calculations for all the P states considered.

The $E^{(4)}_{\rm HQED}$ term in expansion (4) is computed as an expectation value of the following approximate operator derived by Pachucki and Komasa [44, 45]:

$$H_{\rm HQED} = \pi q_0^2 \left(\frac{427}{96} - 2 \ln 2 \right) \sum_{i=1}^{3} \delta(\mathbf{r}_i) \,. \tag{8}$$

$E^{(4)}_{\rm HQED}$ includes the dominant electron–nucleus one-loop radiative correction. The two-loop radiative, electron–electron radiative, and higher-order relativistic corrections are neglected. The above expression only provides a raw estimate of $E^{(4)}_{\rm HQED}$. It seems that, based on the available data for smaller atoms, one can expect that it should capture the bulk of the higher-order QED effects with an overall error that is likely to be less than 50%.

It should be noted that the expectation values of both the $H_{\rm QED}$ and $H_{\rm HQED}$ Hamiltonians are calculated in this work with the infinite-nuclear-mass wave functions, because the corresponding formalism was developed under the assumption of a clamped nucleus [44, 45]. Hence, no recoil effects are included in the $E^{(3)}_{\rm QED}$ and $E^{(4)}_{\rm HQED}$ computed in this work.

Some of the aforementioned operators include singular terms. For instance, $H_{\rm MV}$ contains the terms proportional to $\nabla^4_{\mathbf{r}_i}$ and $H_{\rm D}$, $H_{\rm SS}$, $H_{\rm QED}$, and $H_{\rm HQED}$ include singular one- and two-electron Dirac delta functions, $\delta(\mathbf{r}_i)$ and $\delta(\mathbf{r}_{ij})$ (note that $\delta(\mathbf{r}_i) \equiv \delta(x_i)\delta(y_i)\delta(z_i)$). The expectation values of these operators usually converge rather slowly with the number of the basis functions used to expand the wave function. While there are multiple factors that contribute to the slow convergence, the main reason for this deficiency is related to the fact that with these operators, the expectation values sample the wave function locally (e.g. in the subspace where $\mathbf{r}_i = 0$) rather than globally in the entire coordinate space. The approximate nonrelativistic wave function may have a local error that is considerably more significant than the global error in the energy expectation value, which largely cancels out due to the nature of the variational method (this behavior is general and occurs for any basis set employed). There have been studies that aimed to transform the singular operators to more global operators to accelerate the convergence of the expectation values calculated with those operators with the number of basis functions [46–51]. A rather practical approach was proposed by Drachman [51] based on the work of Trivedi [50]. The Drachman approach has been adopted in quite a few works in recent decades; it makes use of an expectation value identity. For exact eigenfunctions, the approach gives the same expectation values as when the singular (non-global) operator is used. At the same time, for approximate wave functions, as the studies performed so far have demonstrated, the use of the expectation value identity facilitates a considerable improvement of the convergence of the expectation values of the singular operators that appear in the operators representing the leading relativistic corrections [39, 52].

The use of the Drachman method [51] (which may be referred to as a regularization technique) has been very effective not only for Gaussian basis functions but also for other types of function [20, 28]. However, due to the improper behavior of the Gaussian functions (1) in the vicinity of particle coalescence points and due to the fact that they do not satisfy the Kato cusp conditions [53], improving the convergence of the expectation values of singular operators calculated using Gaussians is particularly important. Even though the poor convergence can be remedied to some degree by simply using larger Gaussian basis sets, adopting the regularization technique clearly brings great benefits [51, 52].

Table 2. Convergence of the nonrelativistic variational energy ($E_{\rm nr}$), the mass–velocity correction ($H_{\rm MV}$), and the expectation values of the one- and two-electron Dirac δ-functions with the number of basis functions for the lowest twelve ^2P states of the lithium atom. The numbers in parentheses are estimated uncertainties due to the basis truncation. All values are in atomic units. In references [28, 29] the variational calculations were performed using the Hy-type basis functions.

State	Isotope	Basis	$E_{\rm nr}$	$\langle\tilde{H}_{\rm MV}\rangle$	$\langle\tilde{\delta}(\mathbf{r}_i)\rangle$	$\langle\tilde{\delta}(\mathbf{r}_{ij})\rangle$	$\langle H_{\rm OO}\rangle$	$\langle\mathcal{P}\left(1/r_{ij}^3\right)\rangle$	$E_{\rm tot}$
$1s^22p^1$	^{7}Li	6000	−7.409 557 758 65	−77.480 954	4.557 646 046	0.177 384 817	−0.406 154 192		−7.410 071 856 21
		7000	−7.409 557 758 81	−77.480 940	4.557 646 048	0.177 384 818	−0.406 154 190		−7.410 071 855 77
		8000	−7.409 557 758 95	−77.480 931	4.557 646 050	0.177 384 818	−0.406 154 189		−7.410 071 855 52
		9000	−7.409 557 759 00	−77.480 925	4.557 646 051	0.177 384 818	−0.406 154 189		−7.410 071 855 27
		∞	−7.409 557 7592(1)						−7.410 071 8550(2)
		9000	−7.409 458 110 56	−77.476 815	4.557 465 283	0.177 378 181	−0.407 772 896		−7.409 972 213 63
	^{6}Li	∞	−7.409 458 1108(1)						−7.409 972 2133(2)
	$^\infty$Li	9000	−7.410 156 532 63	−77.505 624	4.558 732 350	0.177 424 700	−0.396 425 741	9.632 11	−7.410 670 588 37
		∞	−7.410 156 5329(1)						−7.410 670 5881(2)
Ref. [28]		33600	−7.410 156 532 652 41(3)	−77.505 616 73(9)	4.558 732 350 19(2)	0.177 424 6999(1)			
$1s^23p^1$	^{7}Li	6000	−7.336 556 363 16	−77.574 185	4.564 054 035	0.177 726 312	−0.427 812 412		−7.337 071 413 37
		7000	−7.336 556 363 59	−77.574 143	4.564 0540 43	0.177 726 313	−0.427 812 401		−7.337 071 412 00
		8000	−7.336 556 363 63	−77.574 121	4.564 054 045	0.177 726 314	−0.427 812 399		−7.337 071 411 07
		9000	−7.336 556 363 69	−77.574 120	4.564 054 045	0.177 726 314	−0.427 812 399		−7.337 071 411 08
		∞	−7.336 556 3639(1)						−7.337 071 4095(8)
	^{6}Li	9000	−7.336 457 285 72	−77.570 013	4.563 873 525	0.177 719 697	−0.429 434 639		−7.336 972 339 19
		∞	−7.336 457 2859(1)						−7.336 972 3374(9)
	$^\infty$Li	9000	−7.337 151 708 58	−77.598 803	4.565 138 855	0.177 766 074	−0.418 062 732	6.988 68	−7.337 666 714 60
		∞	−7.337 151 7088(1)						−7.337 666 7130(8)
$1s^24p^1$	^{7}Li	7000	−7.311 295 101 02	−77.596 593	4.565 703 912	0.177 808 781	−0.433 510 657		−7.311 810 320 77
		8000	−7.311 295 101 52	−77.596 524	4.565 703 924	0.177 808 784	−0.433 510 637		−7.311 810 318 25
		9000	−7.311 295 101 57	−77.596 505	4.565 703 926	0.177 808 784	−0.433 510 635		−7.311 810 317 48
		10 000	−7.311 295 101 64	−77.596 502	4.565 703 927	0.177 808 784	−0.433 510 635		−7.311 810 317 35
		∞	−7.311 295 1021(2)						−7.311 810 3162(6)
Ref. [29]		∞	−7.311 295 101 6176(2)						
	^{6}Li	10 000	−7.311 196 254 24	−77.592 395	4.565 523 453	0.177 802 172	−0.435 133 712		−7.311 711 476 92
		∞	−7.311 196 2547(2)						−7.311 711 4758(6)
Ref. [29]		∞	−7.311 196 254 2635(2)						
	$^\infty$Li	10 000	−7.311 889 060 73	−77.621 182	4.566 788 460	0.177 848 521	−0.423 755 946	6.363 58	−7.312 404 234 87
		∞	−7.311 889 0612(2)						−7.312 404 2338(6)
Ref. [29]		22 302	−7.311 889 060 758 55						
Ref. [29]		∞	−7.311 889 060 7587(2)						
$1s^25p^1$	^{7}Li	7000	−7.299 694 902 00	−77.604 314	4.566 297 869	0.177 837 805	−0.435 573 946		−7.300 210 165 90
		8000	−7.299 694 902 21	−77.604 304	4.566 297 883	0.177 837 806	−0.435 573 942		−7.300 210 165 68
		9000	−7.299 694 902 27	−77.604 296	4.566 297 884	0.177 837 806	−0.435 573 942		−7.300 210 165 38
		10 000	−7.299 694 902 35	−77.604 290	4.566 297 885	0.177 837 806	−0.435 573 941		−7.300 210 165 18
		∞	−7.299 694 9026(1)						−7.300 210 1658(3)

Table 2. Continue

Ref. [29]		∞	−7.299 694 902 339 30(6)						
	^{6}Li	10 000	−7.299 596 170 62	−77.600 184	4.566 117 425	0.177 831 195	−0.437 197 305		−7.300 111 440 44
		∞	−7.299 596 1709(1)						−7.300 111 4399(4)
Ref. [29]		∞	−7.299 596 170 660 65(5)						
	$^{\infty}$Li	10 000	−7.300 288 166 22	−77.628 970	4.567 382 335	0.177 877 536	−0.425 817 528	6.108 29	−7.300 803 387 41
		∞	−7.300 288 1665(2)						−7.300 803 3880(3)
Ref. [29]		22 302	−7.300 288 166 265 05						
Ref. [29]		∞	−7.300 288 166 2651(1)						
$1s^2 6p^1$	^{7}Li	8000	−7.293 427 187 42	−77.607 658	4.566 561 030	0.177 850 526	−0.436 490 373		−7.293 942 466 83
		9000	−7.293 427 187 61	−77.607 653	4.566 561 044	0.177 850 527	−0.436 490 366		−7.293 942 466 96
		10 000	−7.293 427 187 68	−77.607 649	4.566 561 047	0.177 850 527	−0.436 490 365		−7.293 942 466 89
		11 000	−7.293 427 187 78	−77.607 648	4.566 561 049	0.177 850 527	−0.436 490 365		−7.293 942 466 90
		∞	−7.293 427 1880(1)						−7.293 942 4673(2)
Ref. [29]		∞	−7.293 427 187 8104(4)						
	^{6}Li	11 000	−7.293 328 522 01	−77.603 542	4.566 380 594	0.177 843 917	−0.438 113 854		−7.293 843 808 12
		∞	−7.293 328 5223(1)						−7.293 843 8076(2)
Ref. [29]		∞	−7.293 328 522 0817(4)						
	$^{\infty}$Li	11 000	−7.294 020 055 29	−77.632 327	4.567 645 466	0.177 890 254	−0.426 733 210	6.035 59	−7.294 535 292 75
		∞	−7.294 020 0556(1)						−7.294 535 2931(2)
Ref. [29]		22 302	−7.294 020 055 377 65						
Ref. [29]		∞	−7.294 020 055 3779(3)						
$1s^2 7p^1$	^{7}Li	9000	−7.289 662 289 12	−77.609 632	4.566 694 794	0.177 856 934	−0.436 957 281		−7.290 177 588 78
		10 000	−7.289 662 291 25	−77.609 495	4.566 694 848	0.177 856 950	−0.436 957 145		−7.290 177 584 62
		11 000	−7.289 662 291 66	−77.609 377	4.566 694 886	0.177 856 957	−0.436 957 092		−7.290 177 579 71
		12 000	−7.289 662 291 86	−77.609 364	4.566 694 895	0.177 856 958	−0.436 957 083		−7.290 177 579 36
		∞	−7.289 662 2932(7)						−7.290 177 5775(9)
Ref. [29]		∞	−7.289 662 291 990(2)						
	^{6}Li	12 000	−7.289 563 667 15	−77.605 257	4.566 514 443	0.177 850 347	−0.438 580 632		−7.290 078 961 64
		∞	−7.289 563 6686(7)						−7.290 078 9598(9)
Ref. [29]		∞	−7.289 563 667 321(2)						
	$^{\infty}$Li	12 000	−7.290 254 912 62	−77.634 043	4.567 779 296	0.177 896 683	−0.427 199 558	5.910 39	−7.290 770 158 44
		∞	−7.290 254 9140(7)						−7.290 770 1566(9)
Ref. [29]		22 302	−7.290 254 912 797 16						
Ref. [29]		∞	−7.290 254 912 799(2)						
$1s^2 8p^1$	^{7}Li	11 000	−7.287 225 619 01	−77.610 699	4.566 769 796	0.177 860 503	−0.437 219 592		−7.287 740 928 22
		12 000	−7.287 225 620 18	−77.610 694	4.566 769 821	0.177 860 505	−0.437 219 563		−7.287 740 929 16
		13 000	−7.287 225 622 80	−77.610 554	4.566 769 948	0.177 860 533	−0.437 219 301		−7.287 740 925 24
		14 000	−7.287 225 623 27	−77.610 345	4.566 769 963	0.177 860 551	−0.437 219 125		−7.287 740 916 24
		∞	−7.287 225 6241(4)						−7.287 740 9146(8)

Table 2. Continue

Ref. [29]		∞	−7.287 225 623 6354(6)						
	^{6}Li	14 000	−7.287 127 025 81	−77.606 239	4.566 589 512	0.177 853 941	−0.438 842 709		−7.287 642 325 78
		∞	−7.287 127 0266(4)						−7.287 642 3241(8)
Ref. [29]		∞	−7.287 127 026 2255(6)						
	$^{\infty}$Li	14 000	−7.287 818 080 19	−77.635 024	4.567 854 357	0.177 900 275	−0.427 461 394	5.784 97	−7.288 333 331 49
		∞	−7.287 818 0810(4)						−7.288 333 3298(8)
Ref. [29]		22 302	−7.287 818 080 615 15						
Ref. [29]		∞	−7.287 818 080 6158(6)						
$1s^2 9p^1$	^{7}Li	12 000	−7.285 558 671 73	−77.611 430	4.566 814 785	0.177 862 604	−0.437 378 387		−7.286 073 990 66
		13 000	−7.285 558 674 94	−77.611 297	4.566 814 876	0.177 862 633	−0.437 378 126		−7.286 073 987 62
		14 000	−7.285 558 676 57	−77.611 276	4.566 814 921	0.177 862 643	−0.437 378 059		−7.286 073 988 28
		15000	−7.285 558 683 28	−77.611 200	4.566 815 206	0.177 862 671	−0.437 377 805		−7.286 073 991 30
		∞	−7.285 558 6849(8)						−7.286 073 9930(9)
Ref. [29]		∞	−7.285 558 685 6755(5)						
	^{6}Li	15 000	−7.285 460 104 83	−77.607 093	4.566 634 756	0.177 856 061	−0.439 001 410		−7.285 975 419 84
		∞	−7.285 460 1027(9)						−7.285 975 4216(9)
Ref. [29]		∞	−7.285 460 107 2730(5)						
	$^{\infty}$Li	15 000	−7.286 151 025 97	−77.635 879	4.567 899 596	0.177 902 395	−0.427 619 948	5.168 60	−7.286 666 292 31
		∞	−7.286 151 0277(8)						−7.286 666 2940(9)
Ref. [29]		22 302	−7.286 151 028 423 33						
Ref. [29]		∞	−7.286 151 028 4238(5)						
$1s^2 10p^1$	^{7}Li	13 000	−7.284 368 378 68	−77.611 863	4.566 843 800	0.177 863 950	−0.437 479 803		−7.284 883 702 35
		14 000	−7.284 368 383 66	−77.611 544	4.566 843 959	0.177 864 051	−0.437 478 855		−7.284 883 692 52
		15 000	−7.284 368 386 15	−77.611 471	4.566 844 073	0.177 864 068	−0.437 478 715		−7.284 883 691 57
		16 000	−7.284 368 389 00	−77.611 425	4.566 844 119	0.177 864 079	−0.437 478 637		−7.284 883 692 33
		∞	−7.284 368 391(1)						−7.284 883 6934(5)
Ref. [29]		∞	−7.284 368 393 1451(9)						
	^{6}Li	16 000	−7.284 269 824 32	−77.607 318	4.566 663 669	0.177 857 468	−0.439 102 257		−7.284 785 134 65
		∞	−7.284 269 827(1)						−7.284 785 1336(5)
Ref. [29]		∞	−7.284 269 828 5171(9)						
	$^{\infty}$Li	16 000	−7.284 960 648 91	−77.636 104	4.567 928 509	0.177 903 802	−0.427 720 693	5.431 84	−7.285 475 910 55
		∞	−7.284 960 651(1)						−7.285 475 9088(9)
Ref. [29]		22 302	−7.284 960 653 108 64						
Ref. [29]		∞	−7.284 960 653 1095(9)						

Table 2. Continue

$1s^2 11p^1$	^{7}Li	13 000	−7.283 488 879 34	−77.612 374	4.566 861 197	0.177 864 612	−0.437 549 412	−7.284 004 217 67
		14 000	−7.283 488 900 37	−77.611 768	4.566 862 206	0.177 864 894	−0.437 546 891	−7.284 004 209 39
		15 000	−7.283 488 912 02	−77.611 760	4.566 862 672	0.177 864 930	−0.437 546 653	−7.284 004 220 55
		16 000	−7.283 488 924 97	−77.611 725	4.566 862 981	0.177 864 954	−0.437 546 529	−7.284 004 231 79
		∞	−7.283 488 939(7)					−7.284 004 241(5)
	^{6}Li	16 000	−7.28 339 037 060	−77.607 618	4.566 682 529	0.177 858 344	−0.439 170 164	−7.284 596 388 09
		∞	−7.283 390 385(7)					−7.283 905 692(4)
	$^\infty$Li	16 000	−7.28 408 112 297	−77.636 404	4.567 947 381	0.177 904 678	−0.427 788 490	−7.284 596 388 09
		∞	−7.284 081 137(8)				5.197 68	−7.284 596 398(5)
$1s^2 12p^1$	^{7}Li	13 000	−7.282 820 662 48	−77.612 449	4.566 871 208	0.177 865 132	−0.437 595 440	−7.283 335 998 97
		14 000	−7.282 820 702 79	−77.612 128	4.566 872 561	0.177 865 338	−0.437 594 125	−7.283 336 023 22
		15 000	−7.282 820 730 97	−77.612 096	4.566 873 828	0.177 865 421	−0.437 593 890	−7.283 336 049 31
		16 000	−7.282 820 766 49	−77.612 078	4.566 874 695	0.177 865 475	−0.437 593 832	−7.283 336 083 44
		∞	−7.282 820 83(3)					−7.283 336 13(3)
	^{6}Li	16 000	−7.282 722 220 02	−77.607 971	4.566 694 242	0.177 858 865	−0.439 217 485	−7.283 237 543 96
		∞	−7.282 722 29(3)					−7.283 237 60(3)
	$^\infty$Li	16 000	−7.283 412 917 03	−77.636 757	4.567 959 099	0.177 905 199	−0.427 835 690	−7.283 928 192 28
		∞	−7.283 412 98(3)				4.780 42	−7.283 928 24(3)

In this work, in the calculation of the expectation values of the delta functions expressed in terms of the internal coordinates, we employ the following Drachman identities:

$$\langle\psi|\delta(\mathbf{r}_i)|\psi\rangle = \frac{\mu_i}{\pi}\left[\left\langle\psi\left|\frac{E-V}{r_i}\right|\psi\right\rangle - \left\langle\nabla_{\mathbf{r}}\psi\left|\frac{\mathbf{M}}{r_i}\right|\nabla_{\mathbf{r}}\psi\right\rangle\right], \tag{9}$$

$$\langle\psi|\delta(\mathbf{r}_{ij})|\psi\rangle = \frac{\mu_{ij}}{\pi}\left[\left\langle\psi\left|\frac{E-V}{r_i}\right|\psi\right\rangle - \left\langle\nabla_{\mathbf{r}}\psi\left|\frac{\mathbf{M}}{r_{ij}}\right|\nabla_{\mathbf{r}}\psi\right\rangle\right]. \tag{10}$$

In the above expressions, $\mu_{ij} \equiv m_i m_j/(m_i + m_j)$ is the reduced mass, V is the potential energy operator, and E is the variational energy of the state under consideration (the expectation value of $H^{\rm int}_{\rm nr}$). Due to the absence of singular operators on the right-hand sides of expressions (9) and (10), the convergence of these expectation values is considerably faster.

A slow convergence rate with respect to the number of basis function also takes place for $H_{\rm MV}$. In internal coordinates, this operator can be written in the following matrix form:

$$H_{\rm MV} = -\left(\nabla'_{\mathbf{r}}\beta_0\mathbf{J}\nabla_{\mathbf{r}}\right)^2 - \sum_{i=1}^{3}\left(\nabla'_{\mathbf{r}}\beta_i\mathbf{J}_{ii}\nabla_{\mathbf{r}}\right)^2, \tag{11}$$

where $\beta_0 = 1/\sqrt{8m_0^3}$, $\beta_i = 1/\sqrt{8m_i^3}$, $\mathbf{J} = (J \otimes I_3)$, $\mathbf{J}_{ii} = J_{ii} \otimes I_3$, J is a 3×3 matrix with all its elements equal to 1, and J_{ii} is a 3×3 matrix that has only one nonzero element, $(J_{ii})_{ii} = 1$. In the calculations of the expectation value of $H_{\rm MV}$, we adopted the following identity that is applicable to systems with arbitrary masses of constituent particles:

$$\begin{aligned}\langle\psi|H_{\rm MV}|\psi\rangle = &-\lambda^2\langle\psi|(E-V)^2|\psi\rangle\\ &-\lambda^2\langle\psi|(E-V)\left(\nabla'_{\mathbf{r}}\mathbf{B}\nabla_{\mathbf{r}}\right)|\psi\rangle\\ &+\lambda^2\langle\psi|\left(\nabla'_{\mathbf{r}}\mathbf{M}\nabla_{\mathbf{r}}\right)^2|\psi\rangle\\ &+\lambda^2\langle\psi|\left(\nabla'_{\mathbf{r}}\mathbf{M}\nabla_{\mathbf{r}}\right)\left(\nabla'_{\mathbf{r}}\mathbf{B}\nabla_{\mathbf{r}}\right)|\psi\rangle\\ &-\beta_0\langle\psi|\left(\nabla'_{\mathbf{r}}\mathbf{J}\nabla_{\mathbf{r}}\right)^2|\psi\rangle - \sum_{i=1}^{n}\beta_i\langle\psi|\left(\nabla'_{\mathbf{r}}\mathbf{J}_{ii}\nabla_{\mathbf{r}}\right)^2|\psi\rangle.\end{aligned} \tag{12}$$

The parameter λ and the matrix $\mathbf{B} = B \otimes I_3$ in the above formula are chosen in such a way that the element(s) of the diagonal matrix B corresponding to the lightest particle(s) in the system vanish. For instance, if particle k is the lightest in the system (e.g. the particle is an electron) then we have

$$\lambda^2 = \frac{\beta_0^2 + \beta_k^2}{(M)_{kk}^2}, \tag{13}$$

and the diagonal elements of B are;

$$(B)_{ii} = \frac{\beta_0^2 + \beta_k^2}{\lambda^2(M)_{ii}} - (M)_{ii}. \tag{14}$$

When the difference between the mass of the lightest particle (m_k) and the masses of the other particles in the system (m_0 in the present case) is significant, the right-hand side of expression (12) converges to the exact limit considerably faster upon increasing the size of the basis. This will be demonstrated by the data given in the next section.

Table 3. The convergence of the total nonrelativistic energies of the lowest ^2P state of ^{6}Li, ^{7}Li, and $^\infty$Li with the number of ECG basis functions. All energies are in a.u.

Isotope	Basis	$E_{\rm nr}$
^{6}Li	10 000	−7.409 458 110 568 84
	11 000	−7.409 458 110 570 31
	12 000	−7.409 458 110 572 04
	12 500	−7.409 458 110 572 84
	13 000	−7.409 458 110 573 49
	13 500	−7.409 458 110 573 97
^{7}Li	10 000	−7.409 557 759 011 66
	11 000	−7.409 557 759 013 13
	12 000	−7.409 557 759 014 87
	12 500	−7.409 557 759 015 66
	13 000	−7.409 557 759 016 30
	13 500	−7.409 557 759 016 86
$^\infty$Li	10 000	−7.410 156 532 642 47
	11 000	−7.410 156 532 643 98
	12 000	−7.410 156 532 645 74
	12 500	−7.410 156 532 646 55
	13 000	−7.410 156 532 647 20
	13 500	−7.410 156 532 647 70
	13 500[a]	−7.410 156 532 647 90
Ref. [28][b]	33 600	−7.410 156 532 652 41(3)

[a]The variational optimization of the ECG nonlinear parameters is performed for the infinite nuclear mass.
[b]Variational calculations are performed with Hy-type basis functions.

3. Results

The ground state ($1s^22p^1$) of the lithium atom has been studied extensively by various groups over the last two decades [10–28]. Most of these studies reported results concerning only one or a few of the lowest P states, however. Within an explicitly correlated approach, the higher excited states of lithium were studied by the present authors (up to the $1s^210p^1$ state) [27] and Wang *et al* (up to the $1s^210p^1$ state) [29]. In the present calculations of the ^2P states of lithium, the number of ECG basis functions for each state is significantly increased, compared to those used in the previous calculations [27]. Furthermore, the number of computed ^2P states of lithium that we consider is extended to eleven (up to the state $1s^212p^1$). Importantly, in this work, we implemented and used a regularization method for calculating the expectation values of singular operators.

The calculations performed using the regularization method allow the estimation of its efficiency. Two aspects related to the efficiency can be examined. First, the higher excited states normally require the use of more basis functions in the calculations in order to describe the increasing number of radial nodes of the wave function. However, there are practical limits to the number of basis functions one can include in the calculations, which are constrained by the available computational resources. Therefore, the accuracy of the results achieved for the lower states is usually somewhat better than for the higher states, even if more basis functions are used in the calculation of the latter states. This decrease in the accuracy affects the expectation values of such global operators as the Hamiltonian less than the quantities represented by singular operators. When no regularization is employed, the number of converged significant figures in the expectation values of such singular operators is roughly half (or even less) of the number of converged figures in the expectation values of operators representing global quantities.

In table 1, we show the computed expectation values of $H_{\rm MV}$, $\delta(\mathbf{r}_i)$, and $\delta(\mathbf{r}_{ij})$ for three arbitrarily selected states, ($1s^2np^1$ with $n = 2, 7, 12$), along with the highly accurate results of Wang *et al* [28] obtained for the lowest of these states. In this and other tables, as well as in the text, the tilde sign over an operator indicates that the regularization approach was used in the calculation of the expectation value. Let us take a closer look at the results shown in the table. For example, in the expectation value $\langle\tilde{H}_{\rm MV}\rangle$, six significant figures are converged, while in the expectation value $\langle H_{\rm MV}\rangle$ the number of converged figures is only four (or even three), in spite of using a very large basis set. The improvement is even more noticeable for the expectation values of the delta functions. The numbers of converged significant figures in the expectation values $\langle\tilde{\delta}(\mathbf{r}_i)\rangle$ and $\langle\tilde{\delta}(\mathbf{r}_{ij})\rangle$ are ten and nine, respectively, while for $\langle\delta(\mathbf{r}_{ij})\rangle$ and $\langle\delta(\mathbf{r}_{ij})\rangle$, only five significant figures are converged. Similar behavior can be expected for the expectation values of more excited states. For example, in the case of the $1s^212p^1$ state, the highest considered in this work, $\langle\tilde{H}_{\rm MV}\rangle$ is converged to six significant figures.

A comparison of the converged significant figures of the calculated expectation values for the ground and excited states reveals two interesting points about the calculations. First, the results show that the regularization technique employed in this work very effectively increases the convergence rate of the expectation values of singular operators, even for highly-excited states. Second, the number of basis functions used in the excited-state calculations suffices to obtain accurate expectation values, although it is clear that larger basis sets are required to compute the $\langle\tilde{\delta}(\mathbf{r}_i)\rangle$ and $\langle\tilde{\delta}(\mathbf{r}_{ij})\rangle$ expectation values more accurately.

In table 2, we show the nonrelativistic total energy, $E_{\rm nr}$, which is the total energy including the leading relativistic, QED, and HQED corrections, $E_{\rm tot}$, and some other key expectation values obtained for the lowest eleven ^2P states of the lithium atom. The expectation values include the mass–velocity correction $\langle\tilde{H}_{\rm MV}\rangle$, the Dirac delta functions $\langle\tilde{\delta}(\mathbf{r})\rangle$, the orbit–orbit correction $\langle H_{\rm OO}\rangle$, and the Araki–Sucher distribution $\langle\mathcal{P}\left(1/r_{ij}^3\right)\rangle$.

The nonrelativistic energies of the lowest $1s^22p^1$ state and some of the higher excited states ($1s^2np^1 n = 4, \ldots, 10$) can be compared with the values reported by Wang *et al* [28, 29]. For the $1s^22p^1$ state, the value obtained in a basis of 33 600 Hy functions and then extrapolated to an infinite number of functions is −7.410 156 532 652 41(3) hartree. Our energy of −7.410 156 532 63 hartree obtained in the present work using only 9000 ECG basis functions agrees with that value to 11 decimal figures and lies slightly higher. Also, for the same number of basis functions, the computed nonrelativistic energies in this work are nearly as accurate as their results. For instance, the −7.410 156 532 647 379 hartree value for the

Table 4. $2\,^2P \leftarrow n\,^2P$ transition energies of ^{6}Li and ^{7}Li computed using the infinite-nuclear-mass (i) nonrelativistic energies and then gradually corrected by including finite-nuclear-mass effects (f), relativistic corrections, and the QED and HQED corrections. As the QED and HQED Hamiltonians are only valid for an infinite nuclear mass, the corresponding energy corrections are computed using the wave functions obtained in infinite nuclear mass calculations. All values are in cm^{-1}.

Isotope	ΔE	$2\,^2P \leftarrow 3\,^2P$	$2\,^2P \leftarrow 4\,^2P$	$2\,^2P \leftarrow 5\,^2P$	$2\,^2P \leftarrow 6\,^2P$	$2\,^2P \leftarrow 7\,^2P$
^{6}Li	nr(i)	16 022.704 558(1)	21 567.214 090(2)	24 113.315 772(3)	25 489.006 911(4)	26 315.360 093(2)
	nr(f)	16 021.826 832(1)	21 565.981 611(2)	24 111.905 323(2)	25 487.494 996(4)	26 313.785 01(2)
	nr(f) + rel(f)	16 021.581 04(6)	21 565.68 913(2)	24 111.599 032(6)	25 487.183 63(3)	26 313.470 96(2)
	nr(f) + rel(f) + QED(i)	16 021.617 21(7)	21 565.734 58(5)	24 111.647 854(5)	25 487.233 91(3)	26 313.522 061(1)
	nr(f) + rel(f) + QED(i) + HQED(i)	16 021.618 24(7)	21 565.735 89(1)	24 111.649 252(5)	25 487.235 35(3)	26 313.523 52(1)
	Experiment [54][a]	16 021.57(1)	21 565.74(1)	24 111.75(2)	25 487.03(1)	26 313.54(1)
	Experiment [55][b]	16 021.6203(20)[c]	21 565.7323(30)[d]	24 111.6376(40)[e]	25 487.1987(200)[f]	
^{7}Li	nr(i)	16 022.704 558(1)	21 567.214 090(2)	24 113.315 772(3)	25 489.006 911(4)	26 315.360 093(2)
	nr(f)	16 021.952 035(1)	21 566.157 419(3)	24 112.106 520(5)	25 487.710 667(6)	26 314.009 69(3)
	nr(f) + rel(f)	16 021.706 08(4)	21 565.864 98(2)	24 111.800 269(6)	25 487.399 34(3)	26 313.695 68(3)
	nr(f) + rel(f) + QED(i)	16 021.742 31(3)	21 565.910 48(1)	24 111.849 145(5)	25 487.449 674(3)	26 313.746 84(1)
	nr(f) + rel(f) + QED(i) + HQED(i)	16 021.743 29(3)	21 565.911 73(1)	24 111.850 49(5)	25 487.451 06(3)	26 313.748 25(1)
	Experiment [54][a]	16 021.57(1)	21 565.74(1)	24 111.75(2)	25 487.03(1)	26 313.54(1)
	Experiment [56]	16 021.726	21 565.884	24 111.804	25 487.404	26 313.674
	Experiment [55][g]	16 021.725 67(20)[h]	21 566.884 64(30)[i]	24 111.814 99(40)[j]	25 487.392 67(200)[k]	

Isotope	ΔE	$2\,^2P \leftarrow 8\,^2P$	$2\,^2P \leftarrow 9\,^2P$	$2\,^2P \leftarrow 10\,^2P$	$2\,^2P \leftarrow 11\,^2P$	$2\,^2P \leftarrow 12\,^2P$
^{6}Li	nr(i)	26 850.182 914(4)	27 216.059 0(7)	27 477.3165(3)	27 670.3501(1)	27 817.004(4)
	nr(f)	26 848.565 89(5)	27 214.4127(7)	27 475.6490(3)	27 668.667(1)	27 815.309(4)
	nr(f) + rel(f)	26 848.2501(1)	27 214.0928(3)	27 475.330 26(7)	27 668.347(1)	27 814.986(4)
	nr(f) + rel(f) + QED(i)	26 848.302(1)	27 214.1452(4)	27 475.3826(1)	27 668.400(1)	27 815.039(4)
	nr(f) + rel(f) + QED(i) + HQED(i)	26 848.303(1)	27 214.1467(4)	27 475.3841(1)	27 668.401(1)	27 815.041(4)
	Experiment [54][a]	26 847.82(2)	27 214.46(2)	27 475.35(2)	27 668.56	27 815.33(2)
^{7}Li	nr(i)	26 850.182 914(4)	27 216.0590(7)	27 477.3165(3)	27 670.3501(1)	27 817.004(4)
	nr(f)	26 848.796 56(9)	27 214.648(1)	27 475.8869(6)	27 668.907(3)	27 815.551(8)
	nr(f) + rel(f)	26 848.481(1)	27 214.328(3)	27 475.568 15(7)	27 668.587(1)	27 815.228(4)
	nr(f) + rel(f) + QED(i)	26 848.532(1)	27 214.3802(4)	27 475.6206(1)	27 668.640(1)	27 815.281(4)
	nr(f) + rel(f) + QED(i) + HQED(i)	26 848.534(1)	27 214.3816(4)	27 475.6220(1)	27 668.641(1)	27 815.283(4)
	Experiment [54][a]	26 847.82(2)	27 214.46(2)	27 475.35(2)	27 668.56(2)	27 815.33(2)
	Experiment [57]	26 848.749(21)	27 214.601(22)		27 668.861(23)	27 815.488(24)
	Experiment [58]		27 475.850(23)			

[a]The reported values are for the naturally occurring mixture of ^{6}Li and ^{7}Li isotopes.
[b]Values of 14 903.520 341(41) cm^{-1} are used for the gravity centers of $2^2P_{1/2}$ and $2^2P_{3/2}$ with energies of 14 903.296 792(23) and 14 903.632 116(18) cm^{-1} in the transition energy calculations.
[c]The gravity centers of $^2P_{1/2}$ and $^2P_{3/2}$ with energies of 16 021.7796(10) and 16 021.8760(10) cm^{-1}, respectively.
[d]The gravity centers of $^2P_{1/2}$ and $^2P_{3/2}$ with energies of 21 565.9291(15) and 21 565.9692(15) cm^{-1}, respectively.
[e]The gravity centers of $^2P_{1/2}$ and $^2P_{3/2}$ with energies of 24 111.8471(20) and 24 111.8681(20) cm^{-1}, respectively.
[f]The gravity centers of $^2P_{1/2}$ and $^2P_{3/2}$ with energies of 25 487.4142(100) and 25 487.4262(100) cm^{-1}, respectively.
[g]Values of 14 903.871 689(41) cm^{-1} are used for the gravity centers of $2^2P_{1/2}$ and $2^2P_{3/2}$ with energies of 14 903.648 130(23) and 14 903.983 468(18) cm^{-1} in the transition energy calculations.
[h]The gravity centers of $^2P_{1/2}$ and $^2P_{3/2}$ with energies of 16 021.904 870(10) and 16 022.001 270(10) cm^{-1}, respectively.
[i]The gravity centers of $^2P_{1/2}$ and $^2P_{3/2}$ with energies of 21 566.106 070(15) and 21 566.146 170(15) cm^{-1}, respectively.
[j]The gravity centers of $^2P_{1/2}$ and $^2P_{3/2}$ with energies of 24 112.050 670(20) and 24 112.071 770(20) cm^{-1}, respectively.
[k]The gravity centers of $^2P_{1/2}$ and $^2P_{3/2}$ with energies of 25 487.634 870(100) and 25 487.646 870(100) cm^{-1}, respectively.

total infinite-nuclear-mass energy computed by Wang *et al* [26] using 9170 basis functions and the −7.410 156 532 63 hartree value obtained in this work using 9000 ECG basis functions have errors of nearly the same magnitude when compared to the more accurate extrapolated result.

In order to evaluate the efficiency of the ECG basis, additional calculations are performed for the lowest ^2P state. They involved gradually increasing the number of basis functions from 10000 to 13500 ECGs for ^{7}Li and calculating the nonrelativistic energies of ^{6}Li and $^\infty$Li. Table 3 shows the energies obtained from these calculations. As expected, when the basis size increases, the energy continues to decrease. We estimate that, if we had the capability to include 30000+ ECG basis functions in our basis set and optimize them thoroughly, the convergence of the energy would have been similar to that achieved by Wang *et al* using Hy-type

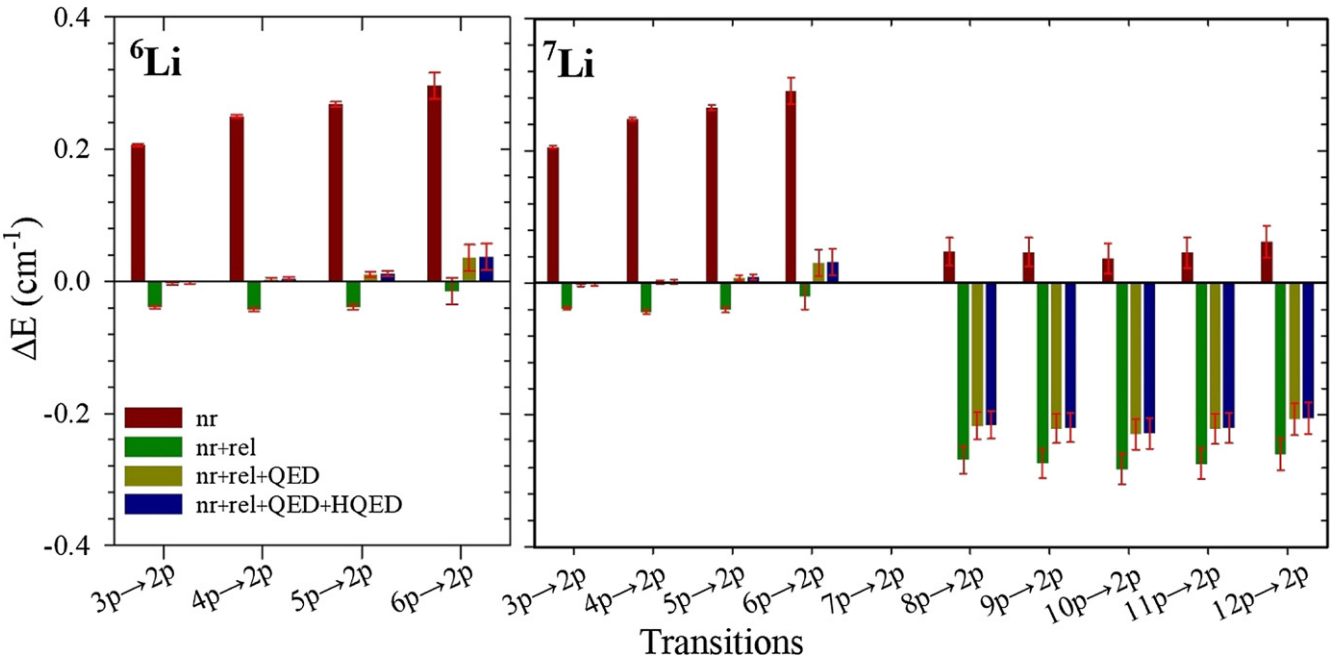

Figure 1. The difference ($\Delta E = \Delta E_{\text{Calculated}} - \Delta E_{\text{Experimental}}$) between the transition energies computed in this work and experimental transitions. For both isotopes, the $2\,^2P \leftarrow n^2P, n = 2, \ldots, 6$ experimental transition energies are taken from reference [55]. The experimental transition energies, of $2\,^2P \leftarrow n^2P, n = 8, \ldots, 12$ of ^{7}Li are taken from references [57, 58]. The calculated transition energies are taken from table 4. The small error bars at the top of each column represent estimated uncertainties in the experimental data. The gravity centers of $^2P_{1/2}$ and $^2P_{3/2}$ have been used for all states.

basis functions. However, this would have required an quantity of computational resources that would have exceeded the amount we were able to allocate for this work. The convergence of the energies in table 3 also demonstrates the importance of optimizing the nonlinear variational parameters of the Gaussian functions. In table 2, we show the energies obtained from our calculations along with the values reported by Wang *et al* in [29]. The values obtained in this work for higher states using more compact wave functions are nearly as accurate as those reported in reference [29], where large Hy-type basis sets of up to 22 302 terms were employed.

Table 4 presents transition energy values calculated using the infinite-nuclear-mass and finite-nuclear-mass nonrelativistic energies, and with energies that include the relativistic, QED, and HQED corrections. The transition energies are calculated with respect to the $1s^22p^1$ state. In addition to the calculated values, some of the relevant experimental results are also shown in the table. These include the measurements of the 31 lowest ^2P states reported by France back in 1930 [54] and the results taken from the following more recent experimental works. We start with the 1959 work of Johansson [56]; in that work, Johansson made some refinements to the energies reported by France. In 1995, Radziemski *et al* [55] made further improvements and reported the transition energies of the ^{6}Li and ^{7}Li isotopes. In 2010, Oxley and Collins [57, 58] reported very accurate measurements of eight ^2P states ($1s^2np^1, n = 8, \ldots, 15$) of the ^{7}Li isotope.

The following observations can be made upon examining the results, including experimental and theoretical data, presented in table 4:

- The transition energies for the lower states reported by Johansson [56], Radziemski *et al* [55], and Oxley and Collins [57, 58] are relatively close to each other. However, the differences between the measured values are larger than the reported uncertainties. Also, the differences between the values reported by France [54] and the values from more recent papers [55–58] are relatively large (about 0.25 cm^{-1}). The results of the four former studies [55–58] are more compatible with each other, thus, as it seems, more reliable, and they are used for comparison with the calculated transition energies in the present work.
- As one can see in the table, the differences between the experimental and nonrelativistic infinite-nuclear-mass computed transition energies (nr(i)) are relatively large and range from 0.5 to 1.25 cm^{-1}. A significant improvement to the results is obtained when the finite mass of the nucleus replaces the infinite mass in the calculations. The replacement causes the difference between the calculated and experimental values to decrease significantly and to range between -0.3 and 0.3 cm^{-1}.
- For ^{6}Li, the only available quality experimental data were reported by Radziemski *et al* [55]. The differences between the calculated transition energies obtained using E_{nr} and the experimental values are relatively large and range from 0.2 to 0.3 cm^{-1}. With the inclusion of the relativistic, QED, and HQED corrections, the differences decrease to 0.045, 0.011, and 0.011 cm^{-1}, respectively. The comparison between the calculated and experimental values is shown in figure 1.

Table 5. Isotope transition-energy shifts of ^{6}Li with respect to ^{7}Li. All values are given in cm^{-1}.

Transition	Basis	(nr)	(nr + rel)	Exp. [55]
$2\,^2P \leftarrow 3^2P$	6000	−0.125 2030	−0.125 2333	−0.1253(10)
	7000	−0.125 2030	−0.125 2334	
	8000	−0.125 2030	−0.125 2334	
	9000	−0.125 2030(1)	−0.125 2334(1)	
$2\,^2P \leftarrow 4^2P$	7000	−0.175 8085	−0.175 8461	−0.1770(30)
	8000	−0.175 8086	−0.175 8462	
	9000	−0.175 8086	−0.175 8462	
	10 000	−0.175 8086(1)	−0.175 8462(1)	
$2\,^2P \leftarrow 5^2P$	7000	−0.201 1964	−0.201 2366	−0.2036(40)
	8000	−0.201 1965	−0.201 2366	
	9000	−0.201 1965	−0.201 2366	
	10 000	−0.201 1965(1)	−0.201 2366(1)	
$2\,^2P \leftarrow 6^2P$	8000	−0.215 6708	−0.215 7121	−0.2207(200)
	9000	−0.215 6708	−0.215 7121	
	10 000	−0.215 6708	−0.215 7121	
	11 000	−0.215 6709(1)	−0.215 7121(1)	
$2\,^2P \leftarrow 7^2P$	9000	−0.224 6817	−0.224 7233	
	10 000	−0.224 6819	−0.224 7237	
	11 000	−0.224 6820	−0.224 7238	
	12 000	−0.224 6820(1)	−0.224 7239(1)	
$2\,^2P \leftarrow 8^2P$	11 000	−0.230 6645	−0.230 7063	
	12 000	−0.230 6645	−0.230 7063	
	13 000	−0.230 6646	−0.230 7065	
	14 000	−0.230 6647(1)	−0.230 7068(2)	
$2\,^2P \leftarrow 9^2P$	12 000	−0.234 8361	−0.234 8780	
	13 000	−0.234 8361	−0.234 8781	
	14 000	−0.234 8361	−0.234 8781	
	15 000	−0.234 8362(1)	−0.234 8782(1)	
$2\,^2P \leftarrow 10^2P$	13 000	−0.237 8592	−0.237 9012	
	14 000	−0.237 8592	−0.237 9015	
	15 000	−0.237 8593	−0.237 9015	
	16 000	−0.237 8593(1)	−0.237 9016(1)	
$2\,^2P \leftarrow 11^2P$	13 000	−0.240 1193	−0.240 1615	
	14 000	−0.240 1192	−0.240 1618	
	15 000	−0.240 1193	−0.240 1619	
	16 000	−0.240 1194(1)	−0.240 1619(1)	
$2\,^2P \leftarrow 12^2P$	13 000	−0.241 8518	−0.241 8942	
	14 000	−0.241 8522	−0.241 8950	
	15 000	−0.241 8523	−0.241 8951	
	16 000	−0.241 8525(1)	−0.241 8952(1)	

- In the case of the less energetic states of ^{7}Li, there have been four experimental reports [55–58]. For the less excited states, the values reported by Johansson [56] and Radziemski *et al* [55] are in full agreement with each other and with the computed values obtained in this work. The calculated differences are very similar to those of

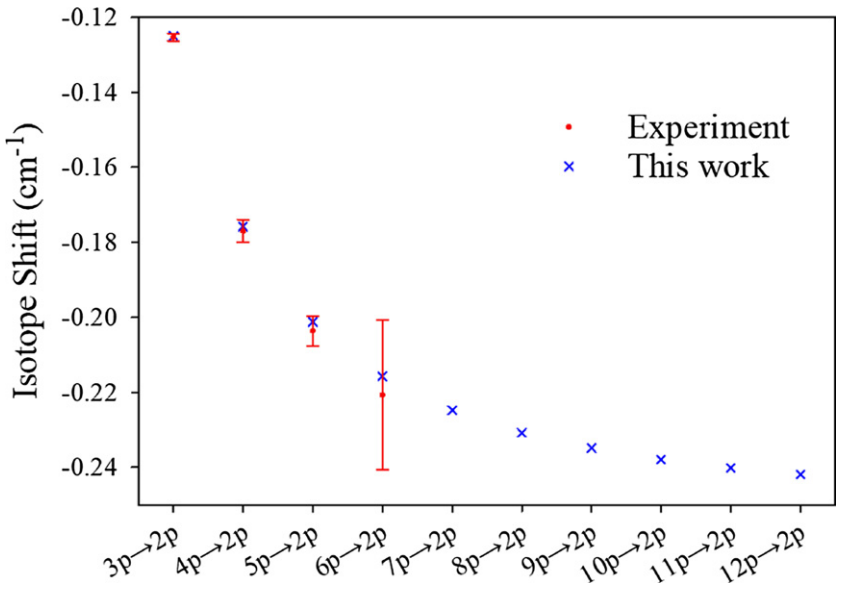

Figure 2. Isotope transition-energy shifts of ^{6}Li with respect to ^{7}Li. The (nr(f) + rel(f)) transition values have been used in the isotope shift calculations. All values are given in cm^{-1}. The experimental isotope shifts are taken from reference [55].

^{6}Li. The inclusion of the relativistic, QED, and HQED corrections significantly improves the agreement with the experimental data and the differences decrease to less than 0.03 cm^{-1}. For the more excited states, the only available values are those reported by Oxley and Collins [57, 58]. Because the two former works [55, 56] have no data in common with the two latter ones, it is not possible to compare the accuracy of the reported data. However, the differences between the transition energies computed in this work and the values reported by Oxley and Collins show a trend that seems contradictory in comparison to the previous papers. For example, the differences between the calculated transition energies using $E_{\rm nr}$ and the experimental values are relatively small (less than 0.09 cm^{-1}). At the same time, inclusion of the relativistic, QED, and HQED corrections significantly increases the differences. Based on the calculated transitions in the present work and on the comparison made above, we believe that the actual uncertainties in the measured values are likely to be larger than the reported uncertainties (see table 4 and figure 1).

- It is worth mentioning that the main sources of error in calculating the transition energies are the QED and HQED corrections. To calculate the QED term, a single approximate value for the Bethe logarithm ($\ln k_0$) is used for all states. This is certainly an approximation. We estimate that the use of a more accurate logarithm value could change the transition energies listed in table 4 by about 0.008 cm^{-1}. The second reason for the error arises from the approximate form of the expression used to compute the HQED expectation value. Here, we roughly estimate that the computed transition energies could change by about 0.0007 cm^{-1} when more accurate HQED correction values become available.

Table 5 shows the isotope shifts in the transition energies determined from the results of our calculations. The experimental data [55] are shown for comparison. In determining the shift values, the non-relativistic (nr) and relativistic corrected (nr + rel) frequencies are used. Comparing the computed and experimental values reveals two key points. First, the computed values, (nr) and (nr + rel), are in full agreement with the experimental values and they are within the uncertainties of the experimental data. Second, the results show that the finite nuclear mass effect is small for less energetic states, but it increases with the excitation level. For instance, the frequency shifts for the lowest transition ($2\ ^2P \leftarrow 3\ ^2P$) are 0.1252030 cm^{-1} (nr) and −0.125 2334 cm^{-1} (nr + rel) while the corresponding values for the $2\ ^2P \leftarrow 12\ ^2P$ transition are −0.241 8518 and −0.241 8952 cm^{-1}, respectively. This is an almost two-fold increase (figure 2).

Finally, in table 6, we show the calculated expectation values of some powers of the inter-particle distances. As expected, both the average nucleus–electron and electron–electron distances increase rapidly with the increasing principal quantum number. It is worth mentioning that the distances differ slightly between the ^{6}Li and ^{7}Li isotopes. The difference originates from the different reduced masses of the electron used in the calculations of the two isotopes. For instance, for the most excited state, the $\langle r_{\rm ne}\rangle$ values for the ^{6}Li and ^{7}Li isotopes are 71.4940 and 71.4934 a.u., respectively. The corresponding values for $\langle r_{\rm ee}\rangle$ are 142.512 and 142.511 a.u., respectively.

4. Summary

The lowest eleven states of the ^2P series ($1s^2np^1$, $n = 2, \ldots, 12$) of the lithium atom were studied using very accurate variational calculations employing explicitly correlated all-electron Gaussian functions. The calculations yielded

Table 6. Expectation values, $\langle r_i^p \rangle$ and $\langle r_{ij}^p \rangle$ ($p = -2, \ldots, 2$) evaluated with the largest basis set generated for each state in this work. All values are in atomic units.

State	Isotope	$\langle r_{ne}^{-2} \rangle$	$\langle r_{ee}^{-2} \rangle$	$\langle r_{ne}^{-1} \rangle$	$\langle r_{ee}^{-1} \rangle$	$\langle r_{ne} \rangle$	$\langle r_{ee} \rangle$	$\langle r_{ne}^{2} \rangle$	$\langle r_{ee}^{2} \rangle$
$1s^2 2p^1$	^{6}Li	9.965 144 85(0)	1.421 642 31(0)	1.879 463 58(0)	0.698 751 993(0)	1.957 237 29(0)	3.470 879 40(0)	9.3171 1136(0)	18.685 1758(0)
	^{7}Li	9.965 409 48(0)	1.421 675 09(0)	1.879 488 08(0)	0.698 759 070(0)	1.957 220 74(0)	3.470 853 27(0)	9.3169 6402(0)	18.684 8879(0)
	$^\infty$Li	9.966 999 63(0)	1.421 872 07(0)	1.879 635 32(0)	0.698 801 595(0)	1.957 121 25(0)	3.470 696 24(0)	9.3160 7855(0)	18.683 1580(0)
$1s^2 3p^1$	^{6}Li	9.954 063 39(0)	1.378 192 89(0)	1.830 186 92(0)	0.599 589 241(0)	4.408 971 09(0)	8.354 992 08(0)	56.508 6959(0)	113.045 290(0)
	^{7}Li	9.954 327 22(0)	1.378 225 13(0)	1.830 211 15(0)	0.599 595 889(0)	4.408 927 01(0)	8.354 911 05(0)	56.507 5879(0)	113.043 082(0)
	$^\infty$Li	9.955 912 57(0)	1.378 418 87(0)	1.830 356 77(0)	0.599 635 838(0)	4.408 662 13(0)	8.354 424 07(0)	56.500 9292(0)	113.029 812(0)
$1s^2 4p^1$	^{6}Li	9.951 603 12(0)	1.367 877 21(0)	1.813 200 64(0)	0.565 471 099(0)	7.861 841 37(0)	15.254 5513(1)	190.909 314(0)	381.839 008(0)
	^{7}Li	9.951 866 77(0)	1.367 909 30(0)	1.813 224 75(0)	0.565 477 510(0)	7.861 756 85(0)	15.254 3894(1)	190.905 244(0)	381.830 876(0)
	$^\infty$Li	9.953 451 02(0)	1.368 102 12(0)	1.813 369 58(0)	0.565 516 032(0)	7.861 248 96(0)	15.253 4164(1)	190.880 786(0)	381.782 009(0)
$1s^2 5p^1$	^{6}Li	9.950 759 07(0)	1.364 256 81(0)	1.805 416 42(0)	0.549 851 804(0)	12.314 9846(0)	24.158 1252(1)	481.587 170(1)	963.191 380(2)
	^{7}Li	9.951 022 66(0)	1.364 288 84(0)	1.805 440 45(0)	0.549 858 084(0)	12.314 8467(0)	24.157 8564(1)	481.576 430(1)	963.169 908(2)
	$^\infty$Li	9.952 606 54(0)	1.3644 8132(0)	1.805 584 87(0)	0.549 895 819(0)	12.314 0177(0)	24.156 2414(1)	481.511 890(1)	963.040 879(2)
$1s^2 6p^1$	^{6}Li	9.950 393 28(0)	1.362 671 11(0)	1.801 215 80(0)	0.541 428 381(0)	17.768 2712(0)	35.063 2747(1)	1017.614 91(0)	2035.245 10(2)
	^{7}Li	9.950 656 84(0)	1.362 703 11(0)	1.801 239 79(0)	0.541 434 582(0)	17.768 0669(0)	35.062 8733(1)	1017.591 58(0)	2035.198 44(2)
	$^\infty$Li	9.952 240 55(0)	1.362 895 42(0)	1.801 383 96(0)	0.541 471 846(0)	17.766 8395(0)	35.060 4612(1)	1017.451 34(0)	2034.918 02(2)
$1s^2 7p^1$	^{6}Li	9.950 209 46(2)	1.361 869 62(3)	1.798 694 71(0)	0.536 375 011(0)	24.221 6686(3)	47.969 2316(5)	1908.069 00(5)	3816.1522(1)
	^{7}Li	9.950 473 00(2)	1.361 901 61(3)	1.798 718 67(0)	0.536 381 163(0)	24.221 3853(3)	47.968 6721(5)	1908.024 42(5)	3816.0631(1)
	$^\infty$Li	9.952 056 64(2)	1.362 093 84(3)	1.798 862 69(0)	0.536 418 124(0)	24.219 6828(3)	47.965 3099(5)	1907.756 52(5)	3815.5273(1)
$1s^2 8p^1$	^{6}Li	9.950 107 06(6)	1.361 4217(1)	1.797 064 04(0)	0.533 107 428(0)	31.675 167(6)	62.875 96(1)	3282.030(1)	6564.073(2)
	^{7}Li	9.950 370 59(6)	1.361 4537(1)	1.797 087 99(0)	0.533 113 545(0)	31.674 793(6)	62.874 95(1)	3281.952(1)	6563.918(2)
	$^\infty$Li	9.951 954 18(6)	1.361 6457(1)	1.797 231 89(0)	0.533 150 299(0)	31.672 545(6)	62.870 50(1)	3281.486(1)	6562.986(2)
$1s^2 9p^1$	^{6}Li	9.950 0454(1)	1.361 1524(9)	1.795 949 01(0)	0.530 873 610(3)	40.128 78(4)	79.782 55(5)	5288.59(1)	10 577.19(3)
	^{7}Li	9.950 3090(1)	1.361 1844(9)	1.795 972 94(0)	0.530 879 700(3)	40.128 31(4)	79.781 62(5)	5288.46(1)	10 576.94(3)
	$^\infty$Li	9.951 8925(1)	1.361 3766(9)	1.796 116 76(0)	0.530 916 290(3)	40.125 48(4)	79.776 00(5)	5287.71(1)	10 575.44(3)
$1s^2 10p^1$	^{6}Li	9.950 0062(2)	1.360 9802(1)	1.795 153 10(0)	0.529 279 407(3)	49.582 48(4)	98.689 71(6)	8096.83(1)	16 193.67(3)
	^{7}Li	9.950 2697(2)	1.361 0122(1)	1.795 177 02(0)	0.529 285 465(3)	49.581 94(4)	98.688 63(6)	8096.65(1)	16 193.31(3)
	$^\infty$Li	9.951 8533(2)	1.361 2043(1)	1.795 320 75(0)	0.529 321 865(3)	49.578 68(4)	98.682 16(6)	8095.55(1)	16 191.11(3)

Table 6. Continue

$1s^2 11p^1$	^{6}Li	9.949 9792(3)	1.360 8658(1)	1.794 565 23(0)	0.528 102 077(8)	60.0368(2)	119.5982(5)	11896.10(9)	23 792.2(2)
	^{7}Li	9.950 2428(3)	1.360 8978(1)	1.794 589 12(0)	0.528 108 084(8)	60.0363(2)	119.5973(5)	11895.88(9)	23 791.8(2)
	$^\infty$Li	9.951 8263(3)	1.361 0898(1)	1.794 732 70(0)	0.528 144 176(8)	60.0334(2)	119.5914(5)	11894.55(9)	23 789.1(2)
$1s^2 12p^1$	^{6}Li	9.949 9583(9)	1.360 7872(2)	1.794 118 71(1)	0.527 207 942(9)	71.4940(8)	142.512(2)	16896.6(4)	33 793.2(9)
	^{7}Li	9.950 2219(9)	1.360 8192(2)	1.794 142 60(1)	0.527 213 941(9)	71.4934(8)	142.511(2)	16896.3(4)	33 792.6(9)
	$^\infty$Li	9.951 8054(9)	1.361 0112(2)	1.794 286 15(1)	0.527 249 985(9)	71.4899(8)	142.504(2)	16894.4(4)	33 788.8(9)

nonrelativistic total energies and the corresponding wave functions for the considered states. The wave functions were used in perturbation-theory calculations of the leading relativistic and QED corrections to the energies of the considered states. The transition energies for the states determined with respect to the lowest $1s^2 2p^1$ state were also calculated. The transition energies were compared with the experimental values. The transition energies obtained using the nonrelativistic energies of the states differed from the most accurate experimental results by less than 0.3 cm^{-1}. The inclusion of the relativistic, QED, and HQED corrections reduced the difference to less than 0.1 cm^{-1}. The transition frequencies determined for ^{6}Li and ^{7}Li were used to calculate the isotopic shifts. The calculated shifts agreed with the available experimental results within the reported experimental uncertainties.

Acknowledgments

This work was supported by Nazarbayev University (faculty development Grant No. 090118FD5345), and the National Science Foundation (Grant No. 1856702).

Data availability statement

All data that support the findings of this study are included within the article (and any supplementary files).

ORCID iDs

Saeed Nasiri https://orcid.org/0000-0001-8501-9859

References

[1] Gallagher T 1994 *Rydberg Atoms* (*Cambridge Monographs on Atomic, Molecular and Chemical Physics* vol 3) (Cambridge: Cambridge University Press)
[2]Šibalić N and Adams C S 2018 *Rydberg Physics* (Bristol: IOP Publishing)
[3] Briegel H-J, Calarco T, Jaksch D, Cirac J I and Zoller P 2000 *J. Mod. Opt.* **47** 415
[4] Feynman R P 1982 *Int. J. Theor. Phys.* **21** 467
[5] Adams C S, Pritchard J D and Shaffer J P 2019 *J. Phys. B: At. Mol. Opt. Phys.* **53** 012002
[6] Saffman M 2016 *J. Phys. B: At. Mol. Opt. Phys.* **49** 202001
[7] Saffman M, Walker T G and Mølmer K 2010 *Rev. Mod. Phys.* **82** 2313
[8] Bubin S, Pavanello M, Tung W-C, Sharkey K L and Adamowicz L 2013 *Chem. Rev.* **113** 36
[9] Rychlewski J 2003 *Explicitly Correlated Wave Functions in Chemistry and Physics: Theory and Applications* (*Progress in Theoretical Chemistry and Physics*) (Dordrecht: Kluwer)
[10] Yan Z-C and Drake G W F 1995 *Phys. Rev.* A **52** 3711
[11] Yan Z-C and Drake G W F 1998 *Phys. Rev. Lett.* **81** 774
[12] King F W 1999 *Advances in Atomic Molecular and Optical Physics* vol 40 ed B Bederson and H Walther (New York: Academic) pp 57–112
[13] Pachucki K 2002 *Phys. Rev.* A **66** 062501
[14] Yan Z-C and Drake G W F 2002 *Phys. Rev.* A **66** 042504

[15] Pachucki K and Komasa J 2003 *Phys. Rev.* A **68** 042507
[16] Drake G W, Nörtershäuser W and Yan Z-C 2005 *Can. J. Phys.* **83** 311
[17] Puchalski M and Pachucki K 2006 *Phys. Rev.* A **73** 022503
[18] Pachucki K and Komasa J 2006 *J. Chem. Phys.* **125** 204304
[19] King F W 2007 *Phys. Rev.* A **76** 042512
[20] Puchalski M and Pachucki K 2008 *Phys. Rev.* A **78** 052511
[21] Yan Z-C, Nörtershäuser W and Drake G W F 2008 *Phys. Rev. Lett.* **100** 243002
[22] Sims J S and Hagstrom S A 2009 *Phys. Rev.* A **80** 052507
[23] Puchalski M, Kędziera D and Pachucki K 2010 *Phys. Rev.* A **82** 062509
[24] Puchalski M and Pachucki K 2010 *Phys. Rev.* A **81** 052505
[25] Wang L M, Yan Z-C, Qiao H X and Drake G W F 2011 *Phys. Rev.* A **83** 034503
[26] Wang L M, Yan Z-C, Qiao H X and Drake G W F 2012 *Phys. Rev.* A **85** 052513
[27] Bubin S and Adamowicz L 2012 *J. Chem. Phys.* **136** 134305
[28] Wang L M, Li C, Yan Z-C and Drake G W F 2017 *Phys. Rev.* A **95** 032504
[29] Wang L, Zhang Y, Sun D and Yan Z-C 2020 *Phys. Rev.* A **102** 052815
[30] Bubin S and Adamowicz L 2006 *J. Chem. Phys.* **124** 224317
[31] Bubin S and Adamowicz L 2008 *J. Chem. Phys.* **128** 114107
[32] Hamermesh M 1962 *Group Theory and its Application to Physical Problems* (Reading, MA: Addison-Wesley)
[33] Pauncz R 1979 *Spin Eigenfunctions* (New York: Plenum)
[34] Caswell W E and Lepage G P 1986 *Phys. Lett.* B **167** 437
[35] Pachucki K 1997 *Phys. Rev.* A **56** 297
[36] Bethe H A and Salpeter E E 1977 *Quantum Mechanics of One- and Two-Electron Atoms* (New York: Plenum)
[37] Akhiezer A I and Berestetskii V B 1965 *Quantum Electrodynamics* (New York: Wiley)
[38] Stanke M, Bubin S and Adamowicz L 2019 *J. Phys. B: At. Mol. Opt. Phys.* **52** 155002
[39] Hornyák I, Adamowicz L and Bubin S 2019 *Phys. Rev.* A **100** 032504
[40] Araki H 1957 *Prog. Theor. Phys.* **17** 619
[41] Sucher J 1958 *Phys. Rev.* **109** 1010
[42] Kabir P K and Salpeter E E 1957 *Phys. Rev.* **108** 1256
[43] Pachucki K 1998 *J. Phys. B: At. Mol. Opt. Phys.* **31** 5123
[44] Pachucki K and Komasa J 2004 *Phys. Rev. Lett.* **92** 213001
[45] Pachucki K 2006 *Phys. Rev.* A **74** 022512
[46] Hiller J, Sucher J and Feinberg G 1978 *Phys. Rev.* A **18** 2399
[47] Drachman R J and Sucher J 1979 *Phys. Rev.* A **20** 442
[48] Drachman R J 1980 *Phys. Rev.* A **22** 1755
[49] Hiller J, Sucher J, Bhatia A K and Feinberg G 1980 *Phys. Rev.* A **21** 1082
[50] Trivedi H P 1980 *J. Phys. B: At. Mol. Phys.* **13** 839
[51] Drachman R J 1981 *J. Phys. B: At. Mol. Phys.* **14** 2733
[52] Pachucki K, Cencek W and Komasa J 2005 *J. Chem. Phys.* **122** 184101
[53] Kato T 1957 *Commun. Pure Appl. Math.* **10** 151
[54] France R W 1930 *Proc. R. Soc.* A **129** 354
[55] Radziemski L J, Engleman R and Brault J W 1995 *Phys. Rev.* A **52** 4462
[56] Johansson I 1959 *Ark. Fys.* **15** 169
[57] Oxley P and Collins P 2010 *Appl. Phys.* B **101** 23
[58] Oxley P and Collins P 2010 *Phys. Rev.* A **81** 024501